Available online at www.sciencedirect.com
ScienceDirect
Applied Mathematical Modelling 32 (2008) 327–340
APPLIED MATHEMATICAL MODELLING
www.elsevier.com/locate/apm

Cluster identification and characterization in the riser of a circulating fluidized bed from numerical simulation results

Luben Cabezas-Gómez [a,*], Renato César da Silva [b], Hélio Aparecido Navarro [c], Fernando Eduardo Milioli [a]

[a] *Departamento de Engenharia Mecânica – Escola de Engenharia de São Carlos – Universidade de São Paulo, Av. Trabalhador Sãocarlense, 400, 13566-590 São Carlos, SP, Brazil*

[b] *Departamento de Ciências Exatas, Campus Três Lagoas, Universidade Federal de Mato Grosso do Sul, Av. Ranulpho Marques Leal, 3484, 79620-080 Três Lagoas, MS, Brazil*

[c] *Departamento de Estatística, Matemática Aplicada e Computação, Instituto de Geociências e Ciências Exatas, Universidade Estadual Paulista, ''Júlio de Mesquita Filho'', Av. 24-A, 1515, Cx. P 178, 13506-700, Rio Claro, SP, Brazil*

Received 1 November 2005; received in revised form 1 October 2006; accepted 6 December 2006
Available online 20 December 2006

Abstract

A methodology of identification and characterization of coherent structures mostly known as clusters is applied to hydrodynamic results of numerical simulation generated for the riser of a circulating fluidized bed. The numerical simulation is performed using the MICEFLOW code, which includes the two-fluids IIT's hydrodynamic model B. The methodology for cluster characterization that is used is based in the determination of four characteristics, related to average life time, average volumetric fraction of solid, existing time fraction and frequency of occurrence. The identification of clusters is performed by applying a criterion related to the time average value of the volumetric solid fraction. A qualitative rather than quantitative analysis is performed mainly owing to the unavailability of operational data used in the considered experiments. Concerning qualitative analysis, the simulation results are in good agreement with literature. Some quantitative comparisons between predictions and experiment were also presented to emphasize the capability of the modeling procedure regarding the analysis of macroscopic scale coherent structures.
© 2007 Elsevier Inc. All rights reserved.

Keywords: Clusters; Numerical simulation; Gas–solid flow; Circulating fluidized bed

1. Introduction

In fluidization systems a high quantity of particles forms agglomerates or clusters, defined as regions characterized by high particle concentration in relation to the mean solids concentration in the riser column. These groups of particles move as a single body with little internal relative movement [1]. According to Horio and

* Corresponding author.
E-mail addresses: lubencg@sc.usp.br (L. Cabezas-Gómez), rcsilva@ceul.ufms.br (R.C. da Silva), helio@rc.unesp.br (H.A. Navarro), milioli@sc.usp.br (F.E. Milioli).

0307-904X/$ - see front matter © 2007 Elsevier Inc. All rights reserved.
doi:10.1016/j.apm.2006.12.005

Nomenclature

C_{Ds}	drag coefficient for a single particle in an infinite medium
d_p	particle diameter (m)
g	gravity acceleration (m/s^2)
G	solid elasticity modulus (N/m^2)
P	gas pressure (Pa)
Re_s	Reynolds number based on particle diameter
R_g	ideal gas constant (kJ/kg K)
t	time (s)
v_g and v_s	control volume average velocities, (m/s)
β	interface drag function (kg/m^{2}s)
μ	dynamic viscosity (kg/ms)
α_g and α_s	volumetric fractions
ρ_g and ρ_s	densities (kg/m^3)
σ	standard deviation
τ_g and τ_s	viscous stress tensors (Pa)
ϕ_s	particle sphericity

Subscripts
(g) and (s) gas and solid phases

Clift [2], agglomerates are groups of particles joined together by the action of inter-particle forces, and clusters are groups of particles joined together as a result of hydrodynamic effects. However, in several articles in the literature the term ''agglomerate'' is used to refer to clusters.

Another important aspect is cluster shape. Horio and Kuroki [3] found that clusters are structures with a parabolic geometrical shape in the down region and a gas wake in the upper part. Hori and Kuroki conducted a three-dimensional visualization study of the gas–solid flow using a laser sheet technique. On the basis of some research in the literature, Davidson [4] affirms that clusters are groups of particles in the form of vertical sheets with a small width/height ratio, which are coherent during a considerable traveling distance. Büssing and Reh [5] indicate that clusters are non-spherical aggregates with a length/diameter ratio of up to 10, contrary to the descriptions of Horio's group [3,6]; and others).

Regarding this discrepancy, Lackermeier et al. [7] noted that the laser sheet technique used by Horio and coworkers enables only images external to the flow to be obtained, thereby restricting observations to those of very small solid volumetric fractions (mass flow rates from about 0.01 to 0.05 kg/(m^{2}s)). Lackermeier et al. [7] applied Horio's technique, but took a shot of the internal flow through the use of an endoscope observation technique. This technique allowed studying gas–solid flows with solid concentrations characteristic of CFB risers. The clusters they observed were very similar to those described by Davidson [4] and Büssing and Reh [5] and also to those presented in the results sections of the present paper.

For studying clusters a number of numerical simulations have been developed. Tsuo and Gidaspow [8] used a traditional two-fluid model of constant viscosity to study the formation of clusters. Various characteristics of the clusters were described, including density, size and flow pattern, and a discussion of the effect of several parameters on processes of cluster formation were presented. The parameters considered were superficial inlet gas velocity, solid mass velocity, particle size, riser diameter, riser height and mixture of fine particles. It was shown that a decrease in mass flow rate and particle size and an increase in superficial inlet gas velocity, mixture of fine particles and column diameter produced a reduction in cluster population. Work similar to that of Tsuo and Gidaspow was developed by a number of researchers using Eulerian–Lagrangean formulations [9–11,1]; and others).

In this paper the methodology of identification and characterization of clusters of Sharma et al. [12] is applied to results of a numerical simulation. The main objective is to characterize the clusters and to better

analyze the obtained simulation results. Sharma et al. [12] presented three different criteria for cluster definition and identification, which were derived from the criteria proposed by Soong et al. [13]. They accounted for four basic cluster characteristics that allow quantifying the influence of flow parameters on these structures. The parameters considered were particle size and gas superficial velocity. Their analyses were of experimental measurements obtained with a capacitance probe, which provided instantaneous local volumetric solid fraction in a 15 cm diameter circulating fluidized bed. Despite the fact that the methodology was first applied to results of experiments [13,14,12], it was also recently applied by Helland et al. [1] and Cabezas-Gómez and Milioli [15] to numerical simulation results. In the last work the authors studied the influence of the drag function on cluster dynamics.

2. Formulation and theoretical procedure

2.1. Mathematical model

In the present work the hydrodynamic model B for a gas–solid flow developed at IIT (Illinois Institute of Technology) and included in the MICEFLOW code [16] is applied. This model, called the traditional two-fluid model, uses an Eulerian description for each phase, including mass and momentum conservation equations for the phases. To obtain the present model the following hypotheses are considered: both phases are assumed to be isothermal at 300 K; no interface mass transfer is assumed; the solid phase is characterized by a mean particle diameter, density and sphericity factor; both phases are continuous assuming a single gas phase (air) and a single solid phase (glass beads). A detailed descriptions about the average procedure used to obtain the following two-phase gas–solid model are presented in Gidaspow [17] and Enwald et al. [18]. Other works [19–22]; among others) also present the deduction of gas–solid multiphase mathematical models, commonly used for simulating gas–solid flows in fluidization. Next is presented the system of governing equations used in simulations obtained after the averaging process and the constitutive equations modeling.

The continuity equations, representing the mass conservation for gas and solid phases, respectively, are written as

$$\frac{\partial(\rho_g \alpha_g)}{\partial t} + \nabla \cdot (\rho_g \alpha_g \mathbf{v}_g) = 0, \tag{1}$$

$$\frac{\partial(\rho_s \alpha_s)}{\partial t} + \nabla \cdot \rho_s \alpha_s \mathbf{v}_s) = 0. \tag{2}$$

In Eqs. (1) and (2) v_g and v_s represent the velocities (m/s), ρ_g and ρ_s stand are densities (kg/m^3), and α_g and α_s stand for the volumetric fractions of gas and solid phases, respectively. In relation to single-phase continuity equation the above equations differ by the presence of the phases' volumetric fractions. By definition the following relation holds for the volumetric fractions:

$$\alpha_g + \alpha_s = 1. \tag{3}$$

The momentum equations for gas and solid phases, respectively, are expressed as

$$\frac{\partial(\rho_g \alpha_g \mathbf{v}_g)}{\partial t} + \nabla \cdot (\rho_g \alpha_g \mathbf{v}_g \mathbf{v}_g) = -\nabla P + \nabla \cdot (\alpha_g \tau_g) - \beta_B(\mathbf{v}_g - \mathbf{v}_s) + \rho_g \mathbf{g}, \tag{4}$$

$$\frac{\partial(\rho_s \alpha_s \mathbf{v}_s)}{\partial t} + \nabla \cdot (\rho_s \alpha_s \mathbf{v}_s \mathbf{v}_s) = -G\nabla \alpha_s + \nabla \cdot (\alpha_s \tau_s) + \beta_B(\mathbf{v}_g - \mathbf{v}_s) + (\rho_s - \rho_g)\alpha_s \mathbf{g}. \tag{5}$$

In Eqs. (4) and (5), besides the presence of the volumetric fraction of each phase, and the traditional superficial (pressure and viscous forces) and volumetric (gravitational) forces considered for single-phase momentum equations, is also included the term related to the interface momentum transfer. This term is modeled considering the stationary drag function, β, at interface. In the above two equations $\mathbf{g}$ is the gravity acceleration (m/s^2), τ_g and τ_s stand for the viscous stress tensors (Pa), P represents the thermodynamic gas pressure (Pa), G is the solid-phase elasticity modulus (N/m^2) and the subscript B represents the hydrodynamic model B. In this model the gas pressure gradient term it is not present in the solid phase momentum equation, and the

drag function is modified to satisfy the Archimedes' principle and the usual relation for the minimum fluidization [17].

To model the constitutive equations it is assumed a Newtonian rheology and the Stokes hypothesis for both phases, expressing the viscous stress tensor as

$$\tau_g = \mu_g[\nabla \mathbf{v}_g + (\nabla \mathbf{v}_g)^T - \frac{2}{3}(\nabla \cdot \mathbf{v}_g)\bar{\bar{\mathbf{I}}}], \tag{6a}$$

$$\tau_s = \mu_s[\nabla \mathbf{v}_s + (\nabla \mathbf{v}_s)^T - \frac{2}{3}(\nabla \cdot \mathbf{v}_s)\bar{\bar{\mathbf{I}}}]. \tag{6b}$$

For the gas phase the dynamic viscosity μ_g is assumed constant and equal to 1.8×10^{-5} (kg/(m s)). For the solid phase it is also assumed a constant dynamic viscosity value, $\mu_s = 0.509$ (kg/(m s)). This value was obtained from experimental values of axial gas pressure gradients and radial solid volumetric fraction profiles using a momentum balance of the gas–solid mixture in the axial riser direction, integrated in the radial direction (c.f. 8].

The solid phase pressure is modeled empirically through the solid elastic modulus, G, using the empirical correlation of Jayaswal [16] obtained from Mutsers and Rietema [23] data, according to

$$G(\alpha_g) = 10^{-8.686\alpha_g + 6.385}. \tag{7}$$

This correlation computes the solids elasticity modulus in dyn/cm^2. This approach considers only the solid pressure gradient due to particle collisions. In the traditional procedure the kinetic influence is commonly neglected [18].

The stationary drag force at the interface is calculated using the drag function. This function is computed considering the procedure of Gidaspow and coworkers [17], where Ergun [24] correlation is used for $\alpha_s \geqslant 0.2$ and Wen and Yu [25] correlation is used for $\alpha_s < 0.2$.

$$\beta = 150\frac{\alpha_s^2 \mu_g}{\alpha_g^2 (d_p \phi_s)^2} + 1.75\frac{\rho_g \alpha_s |\mathbf{v}_g - \mathbf{v}_s|}{(\alpha_g d_p \phi_s)} \quad \text{for} \quad \alpha_s \geqslant 0.2 \tag{8}$$

and

$$\beta = \frac{3}{4} C_{Ds} \frac{\rho_g \alpha_s \alpha_g |\mathbf{v}_g - \mathbf{v}_s|}{(\alpha_g d_p \phi_s)} \alpha_g^{-2.65} \quad \text{for} \quad \alpha_s < 0.2. \tag{9}$$

In relation (9) C_{Ds} represents the interface drag coefficient for a single particle in an infinite medium, calculated by

$$C_{Ds} = \begin{cases} \dfrac{24}{Re_s}(1 + 0.15 \cdot Re_s^{0.687}) & Re_s < 1000, \\ 0.44 & Re_s \geqslant 1000. \end{cases} \tag{10}$$

The Reynolds number, Re_s, is based on the particle mean diameter d_p, and considers the particle sphericity, ϕ_s:

$$Re_s = \frac{\alpha_g \rho_g |\mathbf{v}_g - \mathbf{v}_s| d_p \phi_s}{\mu_g}. \tag{11}$$

It should be noted that in the traditional model other forces at the interface like the transverse, added mass, history and other forces are commonly neglected. Enwald et al. [18], Fan and Zhu [26] and Crowe et al. [27] present a very detailed review about the formulation of these forces for gas–solids flows modeling.

Finally, the fluidization medium, air, is modeled as an ideal fluid by the ideal gas state equation:

$$\rho_g = P/(R_g T). \tag{12}$$

In Eq. (12) R_g is the ideal gas constant (kJ/kg K). The density of the solid phase, ρ_s, is assumed constant and equal to 2620 kg/m^3. In Eqs. ((1)–(12)) the subscripts (g) and (s) respectively stand for gas and solid phases and t is the time (s).

2.2. Cluster identification and characterization

Soong et al. [13] rely on the following guidelines to define clusters:

- The concentration of solids in the cluster must be significantly higher than the local time-averaged solid concentration at a given local position for a particular set of operational conditions.
- A perturbation in the concentration of solids due to clusters must be higher than the random ground fluctuations of the solid fraction.
- This concentration perturbation should be measured in a sample volume with characteristic length one or two orders of magnitude longer than the particle diameter.

Considering the above, Soong et al. [13] proposed the following criterion: the value of the local instantaneous volumetric solid fraction for a cluster should be higher than its time-averaged value by two times the standard deviation (2σ). This way the clusters can be identified and considered as such when an instantaneous solid fraction exceeds that limit. This criterion was used by Tuzla et al. [14] to detect clusters in a downer fluidized bed. Sharma et al. [12] slightly changed the above criterion on the basis of experimental evidence. In addition to the Soong et al. developments, Sharma et al. [12] proposed the following criteria for cluster life-time:

- The cluster is detected when the instantaneous solid fraction becomes larger than the time-averaged solid fraction plus two times the standard deviation (2σ).
- The starting time of a cluster corresponds to the last time at which the instantaneous solid fraction exceeds the time-averaged solid fraction before satisfying the 2σ criterion.
- The end time of a cluster corresponds to the first time at which the instantaneous solid fraction falls below the time-averaged solid fraction after falling below the 2σ criterion.

The proposition of Sharma et al. [12], denominated as the mean-referenced criterion, renders a cluster duration longer than that provided by the 2σ criterion of Soong et al. Even if the authors recognized that the 2σ criterion is somewhat arbitrary; they observed that the use of a different factor to reduce the influence of background noise (e.g., 3σ) would change results in a quantitative way, but would not change the general dynamic characteristics of the clusters. The arbitrariness of the criterion adopted by Sharma et al. was recently discussed in Cabezas-Gómez and Milioli [15].

After a cluster is identified, its four basic characteristics, as defined by Tuzla et al. [14] and Sharma et al. [12], can be calculated. These characteristics are the mean duration time, the occurrence frequency, the existence time fraction and the mean solid concentration. They are defined as follows:

- Mean duration time (τ_c): the mean time of duration of all clusters in a sample volume. (In Sharma et al. the relevant volume is the volume of the used capacitance probe; when results of simulation are used the relevant volume is that of one computational cell.) Assuming τ_i is the duration time of a single cluster,

$$\tau_c = \frac{\sum_1^n \tau_i}{n}, \tag{13}$$

where n is the total number of clusters detected in the observation period.

- Frequency of occurrence (N_c): the frequency at which the clusters are observed in the sample volume. It is calculated as the mean number of clusters per second that are observed during the entire observation period.
- Existence time fraction (F_c): the fraction of the observation period in which there are clusters in the sample volume.

$$F_c = \frac{\sum_1^n \tau_i}{\tau}. \tag{14}$$

- Mean solid concentration (α_{sc}): the sum of the time-averaged solid fractions for all the clusters over the total number of clusters detected in the observation period, i.e.,

$$\alpha_{sc} = \frac{\sum_1^n \bar{\alpha}_{s,i}}{n}. \tag{15}$$

The above characteristics can also be calculated for cross-sectional average values, i.e.,

$$\langle f \rangle = \frac{1}{2R} \int_0^{2R} f(x)\,dx, \tag{16}$$

where x is the horizontal coordinate direction and $2R$ is the cross-sectional length.

3. Numerical solution strategy

This work uses the MICEFLOW code developed by Jayaswal [16] at the IIT. This program is based on the Syamlal's MULTIFIX code [28], which is an extension of the previous K-FIX code, initially developed for gas–liquid flows [29], and later on adapted to deal with gas–solids flows [30]. K-FIX is based on a numerical method developed by [31] which is an extension of the implicit continuous-fluid Eulerian technique (ICE) developed by [32].

The hydrodynamic conservative system is discretized in finite differences equations that are solved using a point – relaxation technique. The continuity equations are discretized implicitly, while the momentum equations are discretized over a staggered mesh. In the momentum equations the convective terms are treated explicitly and all other terms are treated implicitly. The finite-difference equations are solved in a 2D computational mesh that can be uniform or non-uniform. The scalar variables are set at the center of the cells while the vector variables are placed at the boundaries of the cells.

The overall iterative calculation procedure is as follows (see 16]). The calculations are started with a guessed pressure field that is either the specified initial condition or the pressure field computed in the previous time step. Using this guessed pressure field, the velocities are calculated from the momentum equations. The particulate phase continuity equation is solved using the updated velocities to compute the particulate phase volume fraction. The gas phase volume fraction is then computed. Using the gas volume fraction and updated velocities is computed the gas phase mass residue from continuity equation for gas phase. This residue is used as a convergence criterion. For convergence, the gas pressure is corrected in each cell at a time until convergence is attained or the number of iterations exceeds an inner iteration limit (a number of iterations for one cell at a given time). The computations proceed until the entire computational domain is covered. At the end of such a computational sweep, if a pressure adjustment was necessary in any of the cells, the procedure is repeated until simultaneous convergence in all the cells is obtained. The number of iterations, however, is restricted by an outer iteration limit (i.e., a number of iterations for one time step). The pressure is adjusted in each cell using a combination of Newton's method and the secant method.

In the present simulations were used 5 and 400 for inner and outer iteration limits, respectively. The discretization of convective terms is performed using a first order upwind scheme or donor cell discretization [31,16]. The other terms are discretized with standard centered difference scheme. For temporal integration was used a fixed time step equal to 5×10^{-5} s and the simulation runs until 100 s of fluidization. The minimum gas phase mass residue used for convergence was equal to 10^{-5} (kg/m^3). The MICEFLOW code and versions of this code, as described in this present study, has been widely used in several research works [33,16,34,17]; among others).

4. Simulation setup and initial and boundary conditions

Fig. 1 shows the simulation setup and domain, including the initial, inlet and outlet boundary conditions for both phases. One-dimensional plug flow is assumed at the inlet cross-section. At the outlet the continuity condition is assumed for all variables, except for gas pressure. At the walls the no slip condition is assumed for the gas phase and a partial slip condition is assumed for the solid phase in agreement with Ding and Gidaspow [35]. The value for solid-phase viscosity was taken from Tsuo and Gidaspow [8].

In this work is used a Cartesian coordinate system considering uniform computational mesh in radial direction with 22 cells and non-uniform in axial direction with 297 cells (see Fig. 1).

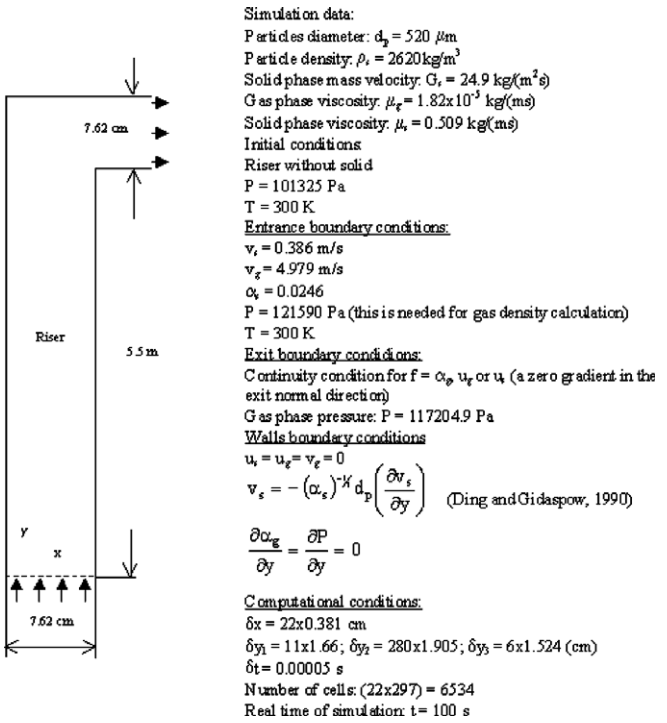

Fig. 1. Geometry and initial and boundary conditions used in the simulations of the IIT installation [42,48] assuming 2D Cartesian coordinates.

Recently Agrawal et al. [36] showed that independent mesh solution for a gas–solid flow is very difficult to be obtained. The cause for this behavior is the meso-scales instabilities that influence and change quantitatively the flow, independently of the adopted temporal and spatial discretizations. These authors affirm that the best form to fully simulate the events taking place at meso and macro scales is the direct numerical integration of the governing equations. However, this kind of simulation, independent of mesh size, was not obtained yet.

In other work, Ibsen et al. [37] studied also a criteria defined Zhang and VanderHeyden [38] concerning the obtainment of grid independent solution. Zhang and VanderHeyden define a grid independent solution as when the flux in the simulation matches the flux in the experiments. Ibsen et al. using this criterion, however, do not obtained a grid independent solution. They pointed out that it is difficult to achieve this kind of solution and that it is questionable whether such a criterion can be satisfied at all when mean volume–length diameter is used.

Considering all the above comments, it seems that the computational mesh used in the present paper leads to satisfactory results. They present physical coherent behavior and acceptable errors in comparison with the experimental data. Similar errors are observed in several works from literature which uses computational meshes similar to the present one [39–41]; among others). The same trends are observed even in works that use more complex mathematical models and refined numerical meshes than the present work (c.f. 37].

5. Numerical results

Introduced in this section is a comparison of numerical results with experimental data, regarding radial profiles of the axial velocity of both phases and of the solid volumetric fraction. Afterwards, the numerical results are analyzed qualitatively applying the clusters' characterization methodology proposed by Sharma et al. [12]. The present results of simulation are compared with the experimental results obtained by those authors.

5.1. Comparison of the numerical results with mean experimental data

In Fig. 2 time averaged radial profiles of the axial gas and solid velocity are compared with the experimental data of Luo [42], 3.4 m above the riser inlet. In Fig. 2a it is observed that significant discrepancies occur between the results of simulation and the experimental data, most significantly in the central region of the column. These deviations can be a consequence of the hypotheses adopted in the employed mathematical model, as well as, due to the experimental uncertainties characteristics of local gas phase velocity measurement. One of the model simplifications is the not consideration of a mathematical model for the gas phase turbulence simulation. The radial profile of the axial solid velocity shows a much more adequate behavior when compared with the experimental data (see Fig. 2b). In this figure it is seen clearly the existence of an annular solid layer with negative velocity in the regions close to the walls. This is evidence of the annular flow pattern characteristic of the gas–solid flow in the upper portions of a riser. It seems that the present model predicts a better solid than gas phase velocity profile, as evidenced in recent publications [43,15,44,45].

The time averaged radial profile of the solid volumetric fraction at 3.4 m above the riser inlet is presented in Fig. 3. The results are qualitatively correct, observing a good agreement between the experimental volumetric fraction and the numerical results. The greater quantitative differences are detected in the region closest to the wall. However, it can be considered that the model produces reasonable qualitative values of the solid volumetric fraction, simulating the annular gas–solid flow pattern with a solid concentration larger at the walls and smaller at the column center. This gas–solid flow pattern is also observed in Fig. 4 where it is shown the instantaneous profiles of the volumetric solid fraction in the entire riser domain in the time interval of 90.0 up to 90.3 s of fluidization. In the figure is perceived clearly the descending movement of a cluster of reasonable size close to the column left wall. This cluster has the form of a vertical sheet with a small width/height ratio, coinciding with the description presented in Davidson [4] and with the structures shown in Lackermeier et al. [7]. It should be noted that this coherent structure is dissipated during its descending movement, having a relatively low velocity, as can be deduced from the results presented in the next section. It is observed that the annular flow pattern is present in almost all the column height.

Others comparisons of the numerical simulation results, obtained with the same mathematical model and the numerical procedure, can be seen in Cabezas-Gómez and Milioli [46,43,15,44,45]. The results here presented show that the model simulates adequately the characteristic behavior of the kind of installation being studied. In spite of this, it is perceived that a more detailed description of the coherent structures' formation, dissipation and breaking dynamics contributes to a better comprehension of the studied gas–solid flow. With this goal, in the following section, simulation results are analyzed using a criterion that allows better quantification of the dynamical processes that characterize these structures.

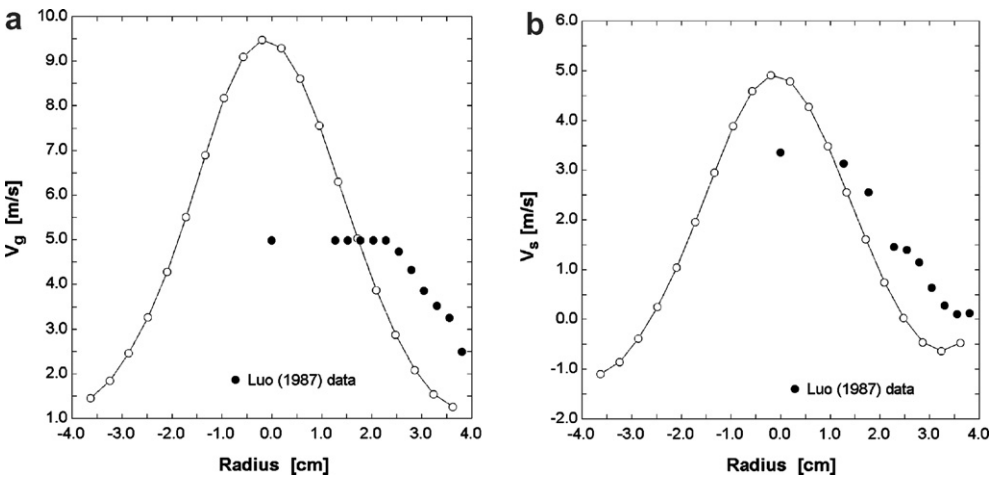

Fig. 2. Time averaged radial profiles of the axial velocity for both phases at 3.4 m height compared with the [42] experimental data.

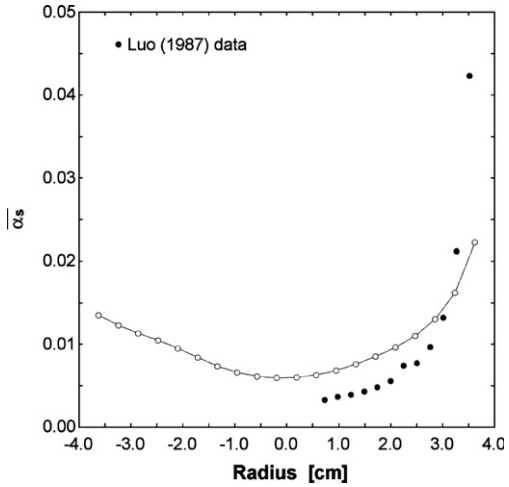

Fig. 3. Comparison of the radial profile of the solid volumetric fraction with the [42] experimental data for the 3.4 m cross section.

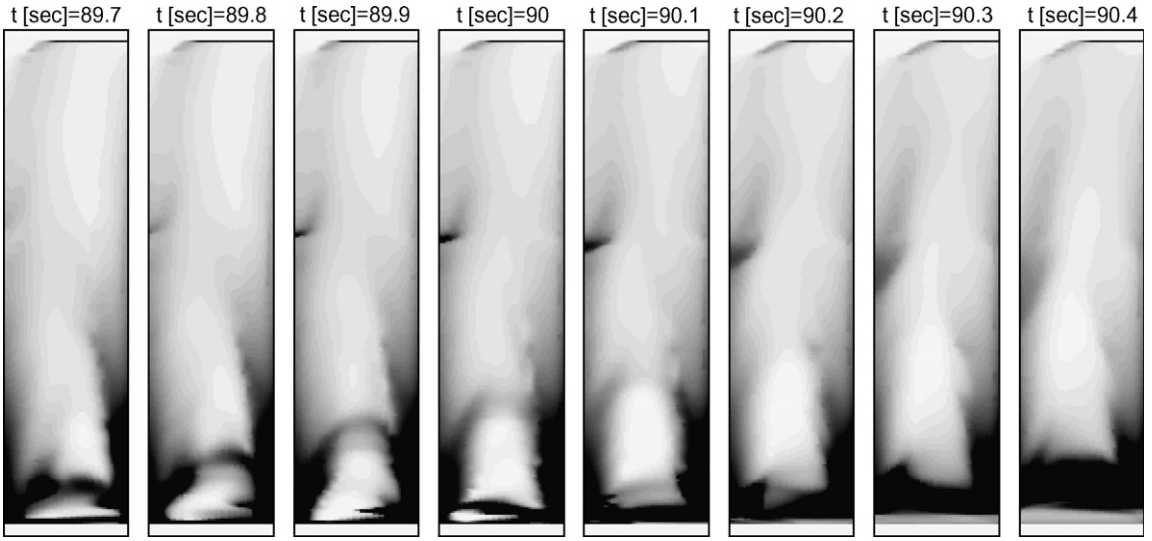

Fig. 4. Temporal photographs of the solid volumetric fraction in the riser column.

5.2. Cluster characteristic analysis from numerical results

The time averaged solid volumetric fraction radial profiles in six bed transversal sections are showed in Fig. 5. The profiles show a similar behavior to each other and in comparison to the experimental data. The only discrepant profile is that corresponding to the height of 5.5 m, next to the riser outlet. In this case it is observed that solids accumulate in the column central region, possible, due to the outlet section geometry (see Fig. 1). This region imposes an obstacle to the flow propitiating the clusters' formation. Except in this riser cross-section, in all the others plotted sections it is seen the gas–solid annular flow pattern. A similar behavior is noted in Fig. 6, regarding the radial profiles of the mean solid concentration in the clusters, α_{sc}. This parameter also shows a solid concentration larger in the regions close to the riser walls. In Fig. 6 it is noted that at the height of 4.5 m the α_{sc} radial profiles already accuse the agglomeration effect exerted by the riser outlet region, while in the profiles for $\bar{\alpha}_s$ this effect is only detected at 5.5 m".

Fig. 7 shows a comparison between the mean cross-sectional time averaged values of the solid volumetric fraction $\langle\bar{\alpha}_s\rangle$, and clusters' solid concentration $\langle\bar{\alpha}_{sc}\rangle$. Both parameters present a similar behavior, with a small

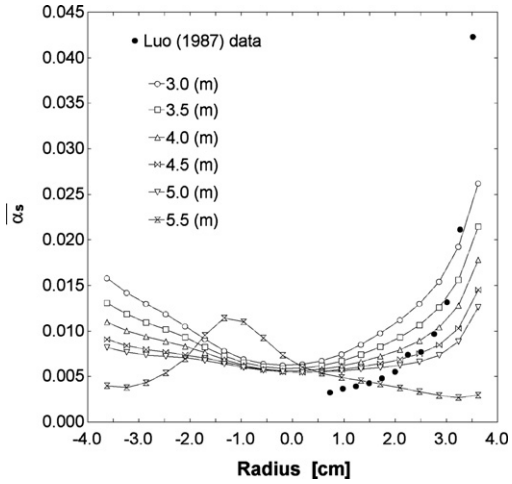

Fig. 5. Time averaged radial profiles of the solid volumetric fraction in several riser cross-sections in comparison with the [42] data obtained at the 3.4 height metres.

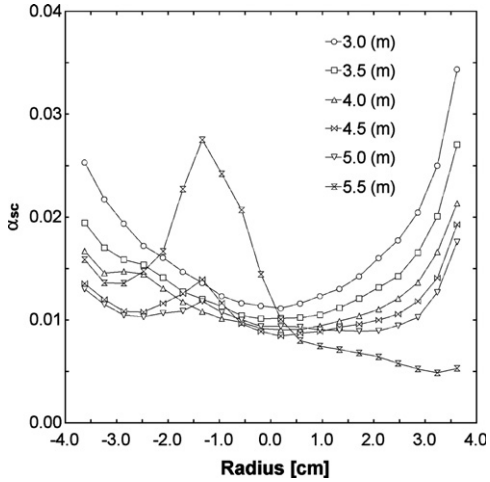

Fig. 6. Radial profiles of the mean cluster solid concentration, α_{sc}, in various riser cross-sections.

difference at height equal to 5.5 m where it is perceived a slight increase of $\langle\bar{\alpha}_{sc}\rangle$ and a diminution of the $\langle\bar{\alpha}_{s}\rangle$ parameter. Once again, this reflects the accumulation of solid with cluster formation in the bed outlet region. Recent works have been show that the inferior region of a CFB behaves as a bubbling fluidized bed (BFB) (e.g 47]. The criteria proposed by Sharma et al. [12] also detect clusters in this region, suggesting the cluster existence even in BFB. This is an interesting aspect that needs more investigation.

The mean cluster duration time, τ_c, is shown in Fig. 8. It is noted a high relative variation among the various radial profiles through the bed, having higher values of τ_c in the regions closer to the column right wall. This does not happen in the left wall, where the profiles are practically plane, showing a slightly increase in some cases. This behavior is caused possibly by the outlet boundary condition and geometry, directing a flow to the right wall and consequently leading to a larger cluster solid concentration in this region. The present results can be compared cautiously with those of Sharma et al. [12] even if both the experimental setups and operating conditions are different and also taking into account that those authors assumed radial symmetry for their experimental results. The comparison is then qualitatively, showing some significant differences. In fact Sharma et al. found the highest value of τ_c equals to 0.15 s at the 4.5 m. In the present work the higher

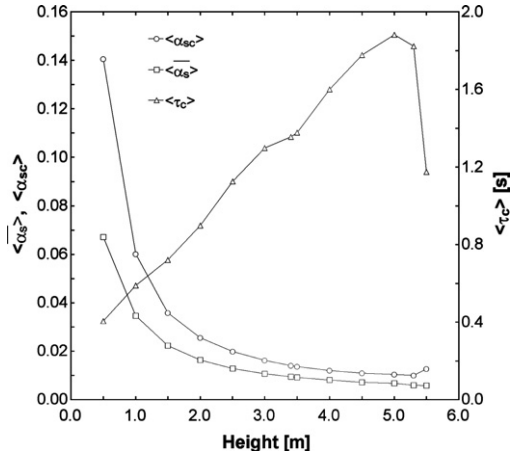

Fig. 7. Comparison of the mean cross-sectional profiles for the time averaged solid concentration, $\langle \bar{\alpha}_s \rangle$, mean cluster solid concentration, $\langle \alpha_{sc} \rangle$, and cluster duration time, $\langle \tau_c \rangle$ along the riser height.

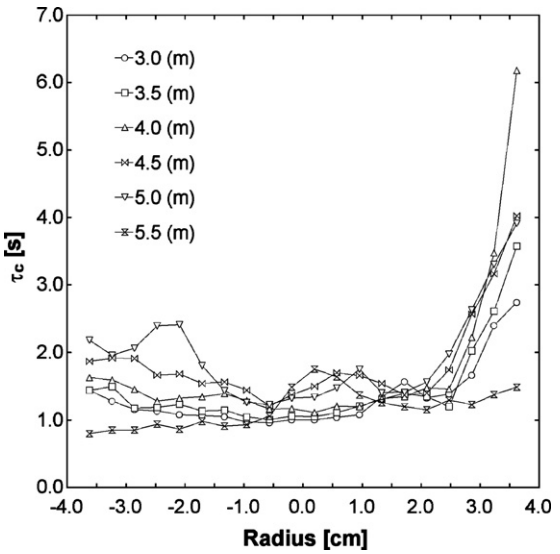

Fig. 8. Radial profiles of the cluster time duration, τ_c, in various riser cross-sections.

value of τ_c at the same height is equal to 4.0 s, indicating that the clusters in the present study have an smaller occurrence frequency and velocity. The reason for this significant difference is not clear but can be related to the different working conditions of the compared installations. More discussion about this fact is presented later in this section.

The mean cross-sectional average value of τ_c, $\langle \tau_c \rangle$, is shown in Fig. 7 as a function or the riser height. The average time of cluster duration is inversely proportional to the solid time average concentrations. Thus, when the clusters are denser, smaller is their duration time for the cross-sectional averaged values. In relation to the properties variation with the riser height it is observed the same behavior show in Figs. 6 and 8. With the height increase $\langle \alpha_{sc} \rangle$ decreases while $\langle \tau_c \rangle$ increases, except at the 5.5 m height where both variables present the same behavior.

In Fig. 9 is shown the radial profiles of the cluster existence time fraction, F_c, and the cluster occurrence frequency, N_c, in several bed transversal sections. In Fig. 9a it is observed a maximum difference of about four times between the obtained F_c values (minimum of 0.06 and maximum of 0.25). However, most of the obtained values oscillate between 0.12 and 0.20. In this figure no functional radial variation of the F_c

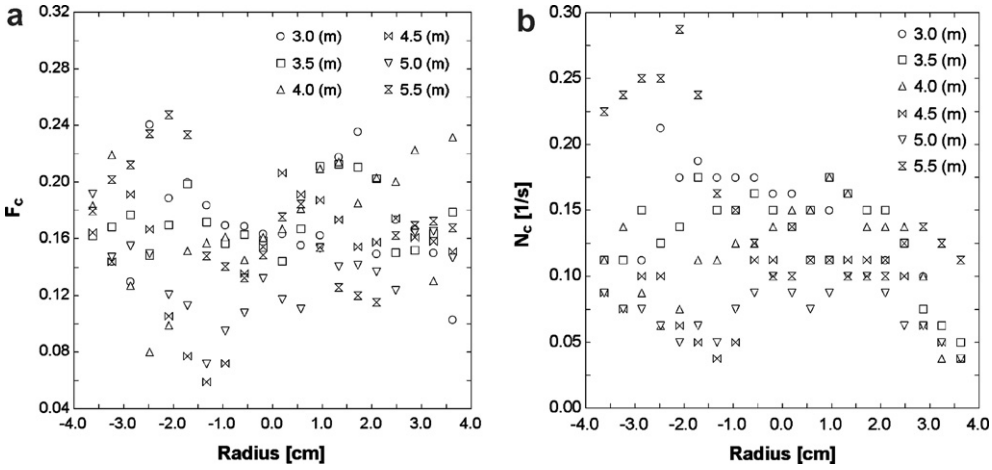

Fig. 9. Radial variation of the clusters' time existence fraction, F_c, and frequency occurrence, N_c, in various riser cross-sections.

parameter is observed at the displayed height cross-sections. In Fig. 9b it can be noticed that the larger frequency of clusters occur for the half to upper riser region takes place at the 5.5 height metres being equal to about 0.30 clusters per second. This value is very low when compared to Sharma et al. data, which is practically equal to 12 cluster per second.

The mean cross-sectional clusters time existence fraction and occurrence frequency for several riser transversal sections are displayed in Fig. 10. The results for the $\langle F_c \rangle$ parameter oscillate in a narrow interval, between 0.13 and 0.20, around an average value of 0.17. This mean cross-sectional average value of $\langle F_c \rangle$ was also obtained by Sharma et al. [12]. According to these authors this value remains almost constant, even when the riser gas superficial inlet velocity and the mean particle diameter are considerably varied. It should be commented that this constancy is, until the present moment, inexplicable. However, considering the definition of F_c it is physically coherent that both the present results and the Sharma et al. [12] experimental data present the same average value. In fact the cluster existence time fraction can be computed as

$$F_c = \frac{\tau_c n}{\tau}. \tag{17}$$

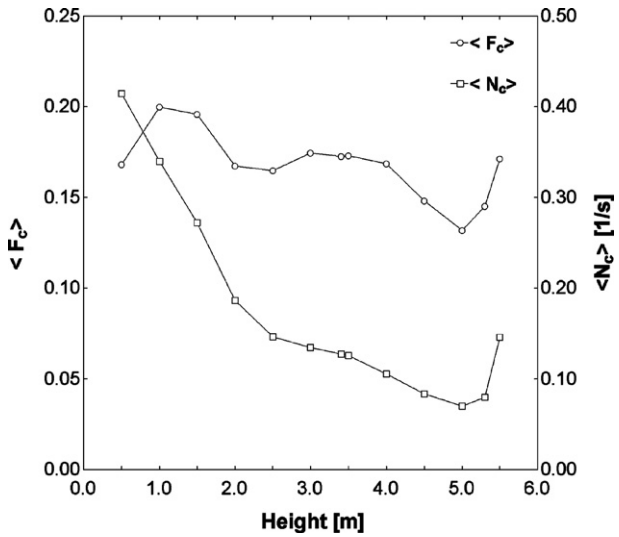

Fig. 10. Cross-sectional mean values of the cluster time existence fraction, $\langle F_c \rangle$, and cluster occurrence frequency, $\langle N_c \rangle$, as a function of riser height.

Eq. (17) physically means that when the number of cluster is high their duration time should be small (Sharma et al. results) and vice-versa if the number of cluster is smaller their duration time should be higher (present simulation). This is because it is not possible, by the adopted cluster definition, to have many clusters with a high duration time in the same place, for a determined cluster observance period τ. In Fig. 10 it is also observed that along the riser column there is a more intense variation of $\langle N_c \rangle$ in comparison to $\langle F_c \rangle$. The higher clusters occurrence frequency is observed at the bottom of the bed, oscillating between 0.13 and 0.41 per second. In the half and upper parts of the column this parameter oscillates between 0.07 and 0.15 per second.

To close this section it can be commented that all the above mentioned differences between the present model results and the experimental data of Sharma et al. [12] can be related to the model assumptions, the uncertainties in the obtainment of experimental data and the differences between the experimental operational conditions and those from numerical simulation. However, deeper studies should be performed to elucidate better the causes of these differences; considering that the clusters' characterization is crucial for good understanding of the complex chemical and hydrodynamics phenomena which take place in a typical CFB installation.

6. Conclusions

In the present paper it is demonstrated that the use of a cluster identification and characterization methodology allows the qualitatively and quantitatively analyze of some hydrodynamics phenomena of the gas–solid riser flows. It was also shown that the present model caught a smaller cluster quantity with a larger duration time in comparison to literature experimental data. The main reason for these discrepancies is not yet well understood, indicating the necessity of more research in this important area. Two possible solutions are the use of a more sophisticated mathematical model, as that based on the kinetic theory of granular flows; and also the development of experimental works considering other techniques for the solid volumetric fraction measurement. Present simulation efforts are under development considering the kinetic theory.

Acknowledgement

The first author fully acknowledges the support received from FAPESP (Fundação de Amparo a Pesquisa do Estado de São Paulo) for the development of this work through a doctoral scholarship (process 98/13812-1).

References

[1] E. Helland, R. Occelli, L. Tadrist, Computational study of fluctuating motions and cluster structures in gas-particle flows, Int. J. Multiphase Flow 28 (2002) 199.
[2] M. Horio, R. Clift, A note on terminology: 'clusters' and 'agglomerates', Powder Technol. 70 (1992) 196.
[3] M. Horio, H. Kuroki, Three-dimensional flow visualization of dilutely dispersed solids in bubbling and circulating fluidized beds, Chem. Eng. Sci. 49 (1994) 2413.
[4] J.F. Davidson, Circulating fluidized bed hydrodynamics, Powder Technol. 113 (2000) 249.
[5] W. Büssing, L. Reh, On viscous momentum transfer by solids in gas–solids flow through risers, Chem. Eng. Sci. 56 (2001) 3803.
[6] M. Tsukada, M. Ito, H. Kamiya, M. Horio, Three-dimension imaging of particle clusters in dilute gas–solid suspension flow, The Can. J. Chem. Eng. 75 (1997) 466.
[7] U. Lackermeier, J. Rudnick, J. Werther, A. Bredebusch, H. Burkhardt, Visualization of flow structures inside a circulating fluidized bed by means of laser sheet and image processing, Powder Technol. 114 (2001) 71.
[8] Y.P. Tsuo, D. Gidaspow, Computation of flow patterns in circulating fluidized beds, AIChE J. 36 (6) (1990) 885.
[9] B.P.B. Hoomans, J.A.M. Kuipers, W.P.M. Van Swaaij, Granular dynamics simulation of cluster formation in dense riser flow, in: 3rd International Conference on Multiphase Flow, Lyon, France, 1998.
[10] J. Ouyang, J. Li, Discrete simulations of heterogeneous structure and dynamic behavior in gas–solid fluidization, Chem. Eng. Sci. 54 (1999) 5427.
[11] E. Helland, R. Occelli, L. Tadrist, Numerical study of cluster formation in a gas-particle circulating fluidized bed, Powder Technol. 110 (2000) 210.
[12] A.K. Sharma, K. Tuzla, J. Matsen, J.C. Chen, Parametric effects of particle size and gas velocity on cluster characteristics in fast fluidized beds, Powder Technol. 111 (2000) 114.
[13] C.H. Soong, K. Tuzla, J. Matsen, J.C. Chen, Identification of particle clusters in circulating fluidized beds, in: Avidan (Ed.), Circulating Fluidized Bed Technology IV Engineering Foundation, New York, p. 615, 1993.

[14] K. Tuzla, A.K. Sharma, J.C. Chen, T. Schiewe, K.E. Wirth, O. Molerus, Transient dynamics of solid concentration in downer fluidized bed, Powder Technol. 100 (1998) 166.
[15] L. Cabezas-Gómez, F.E. Milioli, A numerical simulation analysis regarding the effect of the interface drag function on cluster evolution in a CFB riser gas–solid flow, Braz. J. Chem. Eng. 2 (14) (2004) 569.
[16] U. Jayaswal, Hydrodynamics of Multiphase Flows: Separation, Dissemination and Fluidization. Ph.D. thesis, Illinois Institute of Technology, Chicago, 1991.
[17] D. Gidaspow, Multiphase Flow and Fluidization: Continuum and Kinetic Theory Descriptions, Academic Press, Boston, 1994.
[18] H. Enwald, E. Peirano, A.-E. Almstedt, Eulerian two-phase flow theory applied to fluidization, Int. J. Multiphase Flow 22 (Suppl.) (1996) 21.
[19] T.B. Anderson, R. Jackson, A fluid mechanical description of fluidized beds, Ind. Eng. Chem. Fundam. 6 (1967) 527.
[20] S.L. Soo, Fluid Dynamics of Multiphase System, Blaisdell Inc., Massachusetts, 1967.
[21] D.A. Drew, Mathematical modeling of two-phase flow, Annu. Rev. Fluid Mech. 15 (1983) 261.
[22] R. Jackson, The Dynamics of Fluidized Particles, Cambridge University Press, 2000.
[23] S.M.P. Mutsers, K. Rietema, The effect of interparticle forces on the expansion of a homogeneous gas-fluidized bed, Powder Technol. 18 (1977) 239.
[24] S. Ergun, Fluid flow through packed columns, Chem. Eng. Progr. 48 (2) (1952) 89.
[25] C.Y. Wen, Y.H. Yu, Mechanics of fluidization, Chem. Eng. Progr. Symp. Ser. 62 (62) (1966) 100.
[26] L.S. Fan, C. Zhu, Principles of Gas–Solid Flows, Cambridge University Press, United Kingdom, 1998.
[27] C. Crowe, M. Sommerfeld, Y. Tsuji, Multiphase Flows with Droplets and Particles, CRC Press, Boca Raton, 1998.
[28] M. Syamlal, Multiphase Hydrodynamics of Gas–Solids Flow. Ph.D. thesis, Illinois Institute of Technology, Chicago, 1985.
[29] W.C. Rivard, M.D. Torrey, K-FIX: A Computer Program for Transient Two-dimensional, Two-fluid Flow, Los Alamos, Report LA-NUREG-6623, 1977.
[30] B. Ettehadieh, Hydrodynamic Analysis of Gas–Solid Fluidized Beds. Ph.D. thesis, Illinois Institute of Technology, Chicago, 1982.
[31] F.H. Harlow, A.A. Amsden, Numerical calculation of multiphase fluid flow, J. Comput. Phys. 17 (1975) 19.
[32] F.H. Harlow, A.A. Amsden, A numerical fluid dynamics calculation method for all flow speeds, J. Comput. Phys. 8 (1971) 197.
[33] U.K. Jayaswal, D. Gidaspow, D.T. Wasan, Continuous separation of fine particles in nonaqueous media in a lamella electrosettler, Sep. Technol. 1 (1990) 3.
[34] D. Gisdaspow, J. Ding, U.K. Jayaswal, Multiphase Navier–Stokes equation solver, ASME Numer. Methods Multiphase Flows FED-91 (1990) 47.
[35] J. Ding, D. Gidaspow, A bubbling model using kinetic theory of granular flow, AIChE J. 36 (4) (1990) 523.
[36] K. Agrawal, P.N. Loezos, M. Syamlal, S. Sundaresan, The role of meso-scale structures in rapid gas–solid flows, J. Fluid Mech. 445 (2001) 151.
[37] C.H. Ibsen, T. Solberg, B.H. Hjertager, Evaluation of a three-dimensional numerical model of a scaled circulating fluidized bed, Ind. Eng. Chem. Res. 40 (2001) 5081.
[38] D.Z. Zhang, W.B. VanderHeyden, High-resolution three-dimensional numerical simulation of a circulating fluidized bed, Powder Technol. 116 (2001) 133.
[39] V. Mathiesen, T. Solberg, B.H. Hjertager, Predictions of gas/particle flow with an Eulerian model including a realistic particle size distribution, Powder Technol. 112 (2000) 34.
[40] L. Huilin, D. Gidaspow, Hydrodynamics of binary fluidization in a riser: CFD simulation using two granular temperatures, Chem. Eng. Sci. 58 (2003) 3777.
[41] L. Huilin, D. Gidaspow, J. Bouillard, L. Wentie, Hydrodynamic simulation of gas–solid in a riser using kinetic theory of granular flow, Chem. Eng. J. 95 (2003) 1.
[42] K.M. Luo, Dilute, Dense-Phase and Maximum Solids–Gas Transport. Ph.D. thesis, Illinois Institute of Technology, Chicago, 1987.
[43] L. Cabezas-Gómez, F.E. Milioli, A parametric study of the gas–solid flow in the riser of a circulating fluidized bed through continuous Eulerian modeling, Powder Technol. 132 (2003) 216.
[44] L. Cabezas-Gómez, F.E. Milioli, Collisional solid pressure impact on numerical results from a traditional two-fluid model, Powder Technol. 149 (2–3) (2005) 78.
[45] L. Cabezas-Gómez, F.E. Milioli, Numerical simulation of fluid flow in CFB risers – a turbulence analysis approach, J. Braz. Soc. Mech. Sci. Eng. v.XXVII (2) (2005) 141.
[46] L. Cabezas-Gómez, F.E. Milioli, Gas–solid two-phase flow in the riser of circulating fluidized bed: mathematical modeling and numerical simulation, J. Braz. Soc. Mech. Sci. XXII (2) (2001) 179.
[47] F. Johnsson, R.C. Zijerveld, J.C. Schouten, C.M. van den Bleek, B. Leckner, Characterization of fluidization regimes by time-series analysis of pressure fluctuations, Int. J. Multiphase Flow 26 (4) (2000) 663.
[48] Y. Tsuo, Computation of Flow Regimes in Circulating Fluidized Beds. Ph.D. dissertation, Illinois Institute of Technology, Chicago, 1989.